PHASE-FIELD SIMULATIONS OF BAINITIC PHASE TRANSFORMATION IN 100CR6

Wenwen Song Ulrich Prahl Wolfgang Bleck Krishnendu Mukherjee
Department of Ferrous Metallurgy, RWTH Aachen University, Aachen 52072, Germany

Key words: Microstructure evolution, Phase-field, Bainite, interface mobility

Abstract

Bainitic structure is of considerable importance in the design of high strength steels for application in fatigue loading condition. In order to better understand the mechanisms of bainitic structure formation and to model its microstructure evolution, 2D phase-field simulations were performed coupled with CALPHAD method. In the present work, high carbon bearing steel EN DIN 100Cr6 was used to investigate the bainite transformation. The bainitic growth mode is considered to be faceted in the phase-field simulations. The simulations show the bainitic microstructure evolution and predict its growth kinetics. Carbon diffusion as well as the interfacial mobility during bainitic phase transformation are considered in modeling. The phase-field predicted phase fraction and microstructure evolution results are compared against the dilatometry and HRTEM experimental results. The isothermal bainitic phase transformation kinetics is successfully modeled.

1. Introduction

Bainitic structure plays a key role among solid-solid phase transformations and has been much investigated. However, it still remains the least clearly understood among all austenite decomposition reactions. In the recent years, great efforts has been expended on developing the bainitic phase transformation models in order to better understand the mechanisms of bainitic phase transformation and its microstructure evolution. Several empirical and physical models for bainitic transformation kinetics have been developed [1-7], yet quite few bainitic microstructure evolution models were reported.

In the present paper, phase-field method, a powerful tool for predicting microstructural formation during phase transformation is applied to simulate bainitic phase transformation kinetics and its microstructure evolution in high carbon bearing steel 100Cr6. The simulations are performed using MICRESS ® (microstructure evolution simulations software) code. The simulated kinetics

results are validated via experiments. The following discussions presented here will emphasize the influences of austenite/bainite interface mobility on bainitic microstructure evolution and carbon diffusion through the para equilibrium interface during bainitic phase transformation.

2. Basic descriptions of phase-field model

In the present work, the multi-phase field formulation proposed by Steinbach et.al. [8-10] is employed to describe the austenite to bainite transformation kinetics and its microstructure evolution. In this approach, each grain *i* is marked by its own phase-field parameter ϕ_i. If the grain is present at location *r* and time *t*, the phase-field parameter ϕ_i is marked with $\phi_i(r,t)=1$. If the grain is not present at location *r* and time *t*, the phase-field parameter ϕ_i is marked with $\phi_i(r,t)=0$. The change rate of each phase-field parameter is given by superposition of pairwise interaction with neighboring grains [10]:

$$\frac{d\phi_i}{dt} = \sum_j \mu_{ij}\left[\sigma_{ij}\left(\phi_i\nabla^2\phi_j - \phi_j\nabla^2\phi_i + \frac{\pi^2}{2\eta_{ij}^2}\left(\phi_i - \phi_j\right)\right) + \frac{\pi}{\eta_{ij}}\sqrt{\phi_i\phi_j}\,\Delta G_{ij}\right] \tag{1}$$

where μ_{ij} is the interfacial mobility, σ_{ij} is the interfacial energy, η_{ij} is the interfacial thickness and ΔG_{ij} is driving pressure.

In the present work, bainitic transformation is assumed to take place under para equilibrium condition. Only carbon as an interstitial can redistribute by long-range diffusion, whereas substitutional alloy elements, e.g. Mn, Cr, are considered to be frozen in their sublattice. The composition *c* in $\Delta G(c, T)$ is then represented by the local carbon concentration, *c*, which can be gained by coupling the phase field equation (1) with the carbon diffusion equation. The carbon diffusion is expressed as the sum of the fluxes in the individual grains *i* and *j* weighted by the phase field parameters ϕ_i and ϕ_j with $\phi_i + \phi_j = 1$. The fluxes are calculated from the composition gradient and the diffusivity in each grain, D_i^C and D_j^C [11]:

$$\frac{\partial C}{\partial t} = \nabla\left[\phi_i D_i^C \nabla C_i + \phi_j D_j^C \nabla C_j\right] \tag{2}$$

Where C_i and C_j are the carbon concentration in grain *i* and *j*, respectively.

3. Experimental

The material used in this study was high carbon bearing steel DIN 100Cr6 and its chemical composition is listed in Table 1. The heat treatment was performed in a Bähr 805A dilatometer. A solid cylindrical sample of 3 mm diameter and 10 mm height was used for heat treatment. The specimen was austenitized at 850 °C for 5 min and rapidly quenched to 260 °C. At 260 °C the sample was held isothermally for 2500 s to form bainite.

Table 1. Chemical composition of the investigated steel 100Cr6

Element	C	Si	Mn	P	S	Cr	Mo	Ni	Cu	Al
wt.%	0.967	0.30	0.23	0.003	<0.001	1.38	0.02	0.07	0.05	0.026

To clearly characterize the bainitic microstructure, Tecnai F20G^2 High Resolution Transmission Electron Microscopy (HRTEM) embedded with US1000 Gatan camera and EDX were used. The point resolution of the HRTEM is 0.20 nm. HRTEM foils were prepared from the heat-treated specimen with a twin-jet electro polishing device, using an electrolyte composed of 10 vol.% perchloric acid and 90 vol.% acetic acid. The serving voltage was 58 V.

4. Results and discussions

4.1 HRTEM microstructure analysis

Fig. 1 displays the High Resolution Transmission Electron Microscopy (HRTEM) analysis on bainite microstructure in 100Cr6 isothermally heat treated at 260 °C for 2500 s. To precisely analyze the dimensions of bainite sheaves, more than 100 HRTEM images have been analyzed. A representative for the average bainite sheaf dimensions is shown in Fig. 1. As can be seen in the Fig. 1 (a) and (b), the width of bainite sheaf is around 2.5 μm and the angle of its growth tip is around 30°. In Fig. 1 (a) and (b), the round particles are proved to be $(Fe, Cr)_3C$ using the method of SAD (Selected Area Diffraction). As reported in our previous study [12], $(Fe, Cr)_3C$ is present in 100Cr6 isothermally heat treated at 260 °C for 2500 s. Most of particles are found to be with a width between 0.1 μm to 0.6 μm and the highest size frequency comes up between 0.2 μm to 0.3 μm, which takes up nearly one third of total. Bainite sheaves consist of several bainite ferrite plates, so called bainite subunits, which are shown in Fig. 1 (c).

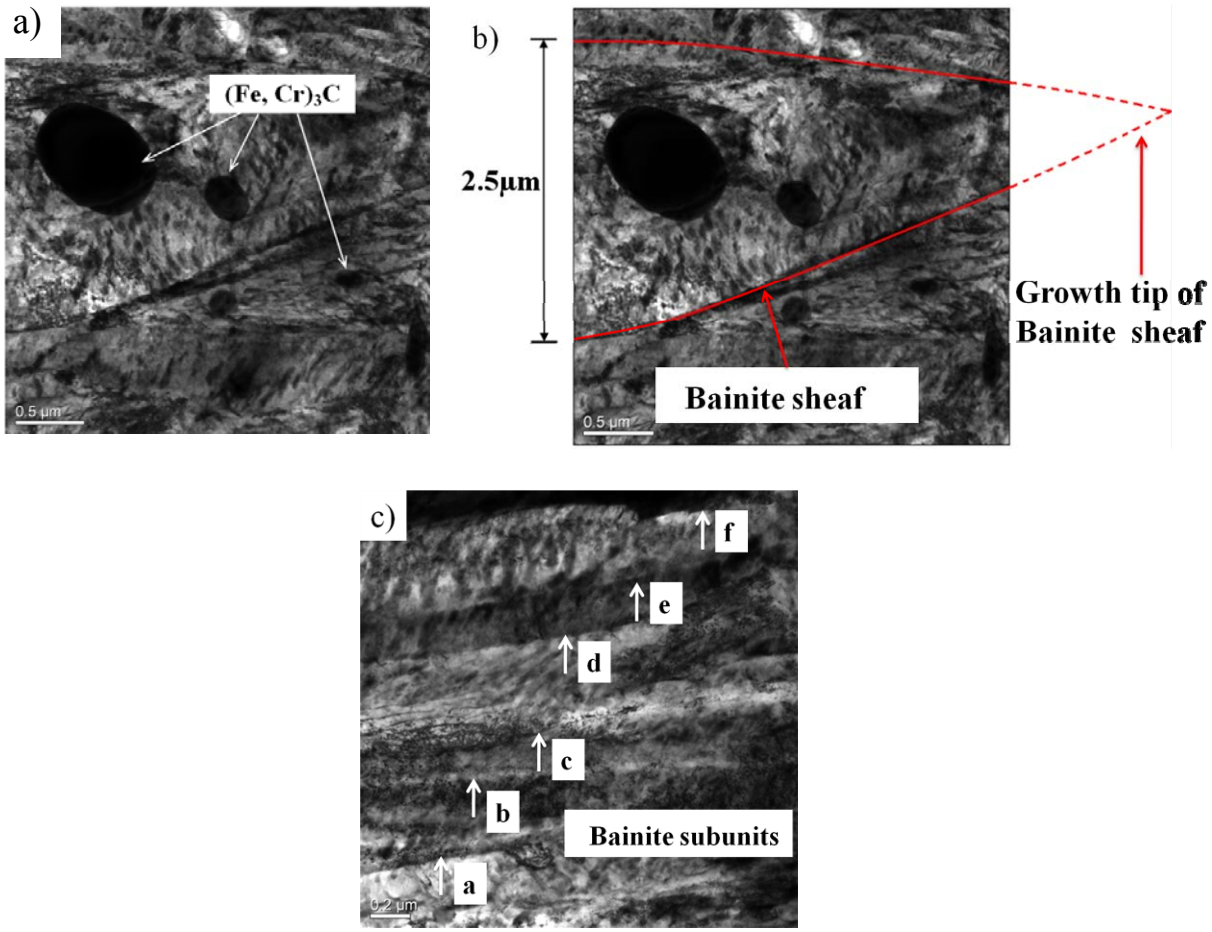

Fig. 1. HRTEM analysis on microstructures in 100Cr6 isothermally heat treated at 260 °C for 2500 s: (a) Bright field HRTEM image showing the $(Fe, Cr)_3C$ (b) Bright field HRTEM image showing the bainite sheaf and its growth tip (c) Bright field HRTEM image showing the bainite subunits a, b, c, d, e, f.

4.2 Phase-field simulations on bainitic microstructure evolution and tranformaion kinetics

Bainite structure is self accommodated which means that its main structure and substructures have quite similar morphologies, yet only the dimensions of the substructures are smaller. Bainite consists of bainite sheaves which again consist of bainite subunits, whereas the morphology of bainite subunits and bainite sheaves are quite similar, which is also illustrated in Fig. 1. Thus in the present work, a single bainite sheaf is chosen to be simulated by means of phase-field approach. The parameters applied for the phase-field simulations of bainitic phase transformation are listed in Table 2. To compare with the HRTEM experimental results, isothermal bainitic transformation at 260 °C is modelled. The bainitic growth is considered to be faceted mode. The width of the bainite sheaf is set according to the HRTEM results. The length of the bainitic sheaf is set to be the radius of the prior austenite grain which is obtained from

experiment proved to be 30 μm. The para equilibrium carbon concentrations both in austenite $x_{C,0}^{\gamma/B}$ and in bainite $x_{C,0}^{B/\gamma}$ are calculated using Thermocalc TCFE6. As is shown in Fig. 2, the evolution of a single bainite sheaf during isothermal holding can be successfully simulated by means of phase-field method.

Table 2. Parameters applied in phase-field simulations of bainitic phase transformation in 100Cr6

Parameters	Values / units
Austenite / Bainite interface energy $\sigma^{B/\gamma}$	2.0E-05 J/cm^2
Austenite / Bainite interface mobility $\mu^{B/\gamma}$	3.00E-06 cm^4/(Js)
C diffusion coefficient in austenite D_γ^C	138.72 cm^2/s
Activation energy for carbon diffusion in austenite Q_C^γ	140900 J/mol
C diffusion coefficient in bainite D_B^C	3.1603 cm^2/s
Activation energy for carbon diffusion in bainite Q_C^B	81800 J/mol
carbon concentration in austenite $x_{C,0}^{\gamma/B}$	4.963 wt%
carbon concentration in bainite $x_{C,0}^{B/\gamma}$	7.04E-02 wt%

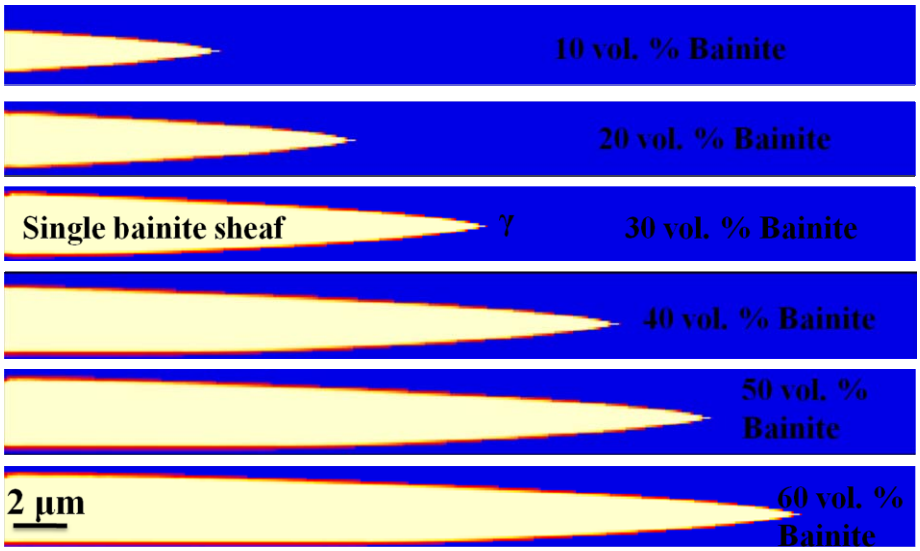

Fig. 2. Phase-field simulation of single bainite sheaf development in 100Cr6 during 260 °C isothermal transformation by means of MICRESS®

Fig. 3 shows the comparison of experimental results and phase-field simulated results of bainitic phase transformation kinetics in 100Cr6 isothermally heat treated at 260 °C for 2500 s. Two results have a satisfactory agreement. It is worth noticing that the austenite / bainite interface mobility $\mu^{B/\gamma}$ applied here is 3.00E-06 cm^4/ (Js).

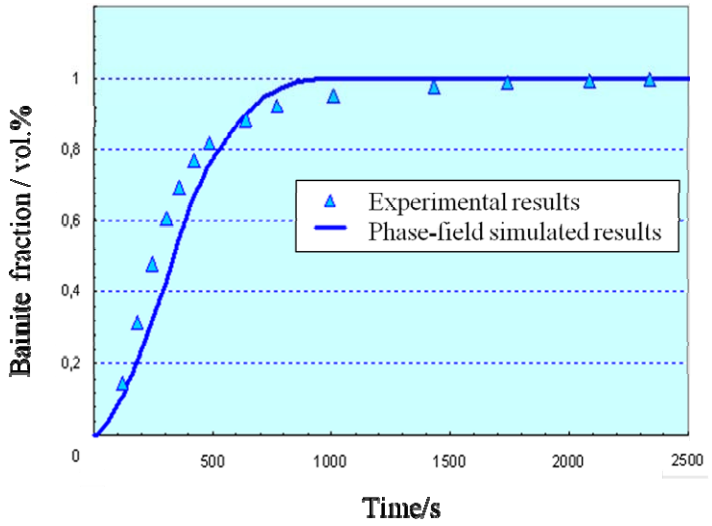

Fig. 3. Comparison of experimental results and phase-field simulated results of bainitic phase transformation kinetics in 100Cr6 during 260 °C isothermal transformation

4.3 Influence of austenite/bainite interface mobility on bainitic phase transformation

Fig. 4 illustrates the influence of interface mobility on bainitic phase transformation kinetics in 100Cr6 during 260 °C isothermal transformation. As is shown in Fig. 4, with the increase of interface mobility $\mu^{B/\gamma}$, bainitic phase transformation becomes faster, whereas the proper value to apply here for bainitic isothermal transformation is 3.00E-06 cm^4/ (Js).

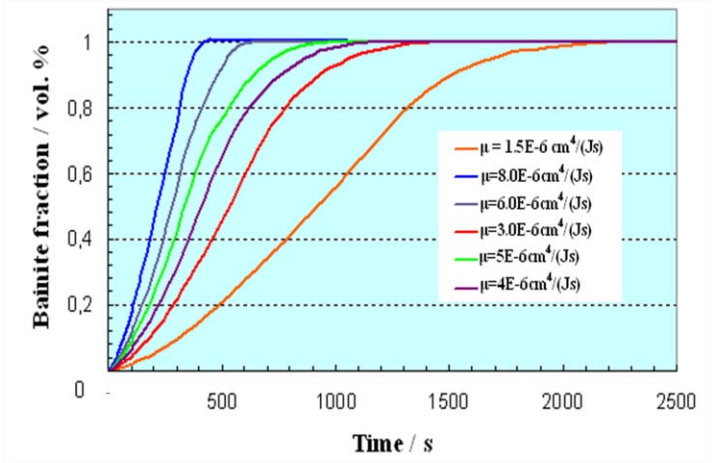

Fig. 4. Influence of interface mobility on bainitic phase transformation kinetics in 100Cr6 during 260 °C isothermal transformation

4.4 Carbon diffusion through austenite/bainite interface

To analyse the carbon diffusion in austenite/bainite interface, the growth tip of bainite sheafis selected which is shown in Fig. 5. The high carbon areas represent the austenite/bainite interface with a certain thickness where carbon atoms diffuse from bainite to austenite during transformation. The carbon concentration along the EDX scanning line in Fig. 6 is shown in Fig. 7. The carbon concentrations in austenite and bainite away from the interface stays the constant, while there exists a peak in the austenite adjacent to the interface, which controls the interface motion and the bainitic phase transformation.

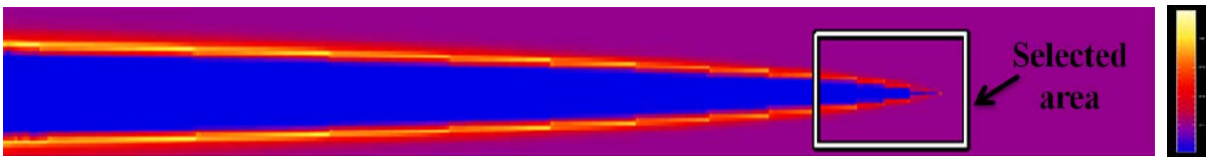

Fig. 5. Carbon profile of 40 vol.% transformed bainite sheaf in 100Cr6 during 260 °C isothermal transformation simulated with phase-field software MICRESS®

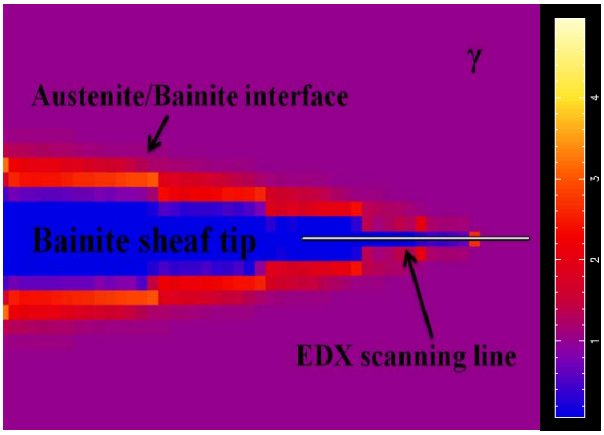

Fig. 6. Carbon profile of selected area, i.e. bainite sheaf tip, in Fig. 5

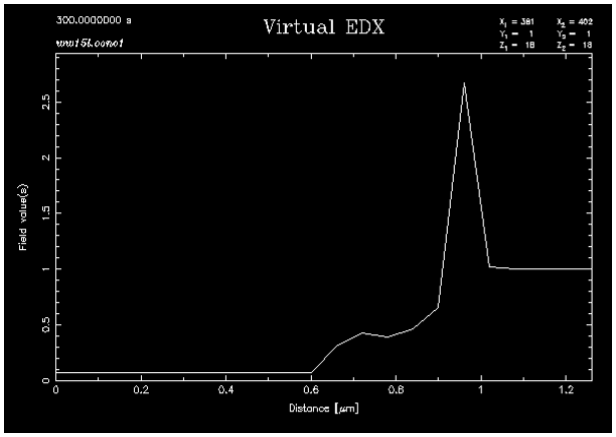

Fig. 7 Virtual EDX showing the carbon concentration along the EDX scanning line in Fig. 6 (carbon content given in wt%)

5. Conclusion

In this work, phase-field simulations, aimed at simulating bainitic phase transformation kinetics and its microstructure evolution was performed. The influence of austenite/bainite interface mobility on bainitic transformation kinetics and carbon diffusions through the para equilibrium interfaces during baintic phase transformation are discussed. With the increase of interface mobility $\mu^{B/\gamma}$, bainitic phase transformation becomes faster, whereas the proper value to apply here for bainitic isothermal transformation is found to be 3.00E-06 cm^4/ (Js). A single bainite

sheaf development during isothermal transformation is successfully simulated by means of phase-field method. The experimental and phase-field simulated results of bainitic phase transformation kinetics have a satisfactory agreement. However, carbides precipitation are not taken into account in the present work. It will be necessary to integrate carbides into phase-field simulations of bainitic phase tranformations in the future.

6. Acknowledgements

The researching work is performed within the project “diffusion controlled bainitic phase transformation” in The Interdisciplinary Centre for Advanced Materials Simulation (ICAMS). Authors would like to express their many thanks to Dr. A.Aghajani in Ruhr-University Bochum for his great support of HRTEM experiment Authors would like to express their many thanks to Dr. A.Aghajani for his great support with the HRTEM experiment.

7. References

[1] S.M.C. Van Bohemen and J. Sietsma Modeling of isothermal bainite formation based on the nucleation kinetics. International Journal of Materials Research **7**, (2008), 739–747.

[2] H.K.D.H. Bhadeshia, Bainite: Overall transformation kinetics. Journal De Physique C4, No. 12, Vol. 43 (1982), 443-448

[3] M. Azuma, et al., Modelling upper and Lower Bainite Transformation in Steels. ISIJ International, 45, (2005), 221-228

[4] P.R. Cha, et al., Phase-field model for multicomponent alloy solidification. Journal of Crystal Growth 274, (2005), 281–293

[5] R.S. Qin and E.R. Wallach, A phase-field model coupled with a thermodynamic database. Acta Materialia 51, (2003), 6199–6210

[6] D. Quidort and Y. Brechet, Isothermal growth kinetics of bainite in 0.5% C steels. Acta Materialia 49, (2001), 4161-4170

[7] C.J. Huang, D.J. Browne and S. McFadden, A Phase-field Simulation of Austenite to Ferrite Transformation Kinetics in Low Carbon Steels, Acta Materialia, 54, (2006), 11-21.

[8] J.Tiaden , B. Nestler and H.J. Diepers, Steinbach I. Phys D1998, 115:73

[9] I. Steinbach, et al., Phys D 1996, 94:135

[10] I. Steinbach, Advances in materials theory and modeling: bridging over multiple length and time scales. San Francisco. (CA): MRS: 2001, AA7.14

[11] M. Militzer, el al., Three-dimensional Phase Field Modelling of the Austenite-to-ferrite Transformation, Acta Materialia, 54 (2006), 3961-3972.

[12] W. Song et al., Modeling of bainitic phase transformation in high carbon steel 100Cr6. International Conference of Advanced steels (ICAS), Guilin,China Nov.9-11, 2010